RSC Advances

PAPER

Published on 24 September 2026
Licensed under CC-BY-NC 4.0

Check for updates

Cite this: *RSC Adv.*, 2026, **16**, 57258

Engineering pectin- and sodium alginate-based nanoemulgels for topical delivery of *Hibiscus sabdariffa* flower extract

Bahruz S. Mammadov,[a] Sevil J. Mehraliyeva,[a] Rukiye Sevinc Özakar,[b] Emrah Özakar,[b] Yasin Bayır,[c] A. Alper Öztürk,[d] Eldar Gasimov[e] and Fuad Rzayev[*f]

Recent advances in nanotechnology have enabled nanoscale topical delivery systems with controlled release and enhanced therapeutic performance. This study developed and evaluated a nanoemulgel incorporating *Hibiscus sabdariffa* L. flower extract obtained *via* high-speed extraction. An oil-in-water nanoemulsion with a mean droplet size of 419.70 ± 46.95 nm, polydispersity index of 0.48 ± 0.05, and zeta potential of −8.10 ± 0.74 mV was successfully prepared, indicating a stable sterically stabilized dispersion. The nanoemulsion was incorporated into pectin- and sodium alginate-based gel matrices to comparatively investigate polymer influence. Rheological analyses revealed pseudoplastic behavior, while morphological characterization by SEM and TEM revealed polymer-dependent matrix structures and approximately spherical nanoscale features in the optimized formulations. FT-IR analysis revealed only minor spectral differences following extract loading, while EDX provided comparative elemental profiles of the optimized formulations. *In vitro* diffusion studies demonstrated controlled and sustained release from both formulations, reaching ≈99% within 24 h. Release kinetic analysis indicated that diffusion may contribute to the release process; however, the kinetic parameters were interpreted primarily as empirical descriptors and were not used to assign a definitive transport mechanism. The sodium alginate-based nanoemulgel (N5) exhibited a comparatively more gradual release profile and a pH of 6.71, supporting its selection for further formulation evaluation. Long-term stability studies per ICH Q1A(R2) and Q1E guidelines showed that N5 maintained physicochemical integrity, colloidal stability, and active content for up to 12 months at 4–8 °C in glass containers, whereas elevated temperatures and plastic packaging caused significant destabilization. Overall, the sodium alginate-based nanoemulgel demonstrated favorable formulation and storage characteristics and represents a promising candidate for further investigation as a topical delivery system for *Hibiscus sabdariffa* extract. Additional studies using validated skin models and appropriate biological evaluations are required to establish its dermal performance and therapeutic applicability.

Received 15th July 2026
Accepted 17th September 2026

DOI: 10.1039/d6ra06448e

rsc.li/rsc-advances

1. Introduction

In recent years, rapid advances in pharmaceutical nanotechnology have profoundly influenced the development of innovative drug delivery systems. Nanotechnology-based drug carriers have been extensively investigated for their ability to improve the solubility of poorly water-soluble compounds, enhance bioavailability, protect labile bioactive molecules, and precisely modulate drug release kinetics. As a result, nanotechnological approaches have found widespread application across various routes of administration, including oral, parenteral, ocular, pulmonary, and dermal delivery systems.[1–5] Within this broad framework, topical and transdermal drug delivery systems have particularly benefited from nanotechnology-driven strategies. Nanoscale carriers can overcome the structural and functional barriers of the skin by improving drug permeation, increasing residence time at the application site, and enabling localized and controlled delivery of active substances. Consequently, nanotechnology-based topical formulations have emerged as promising alternatives to conventional semisolid dosage forms, addressing key

[a]*Azerbaijan Medical University, Department of Pharmaceutical Technology and Management, Baku, AZ1022, Azerbaijan. E-mail: dr.mamedov_86@mail.ru; prof.nanopharmacy@gmail.com*

[b]*Atatürk University, Faculty of Pharmacy, Department of Pharmaceutical Technology, Erzurum, 25240, Türkiye. E-mail: rukiyeso@atauni.edu.tr; emrahozakar@atauni.edu.tr*

[c]*Atatürk University, Faculty of Pharmacy, Department of Biochemistry, Erzurum, 25240, Türkiye. E-mail: ybayir@atauni.edu.tr*

[d]*Anadolu University, Department of Pharmaceutical Technology, Tepebaşı, Eskişehir, 26470, Türkiye. E-mail: aaozturk@anadolu.edu.tr*

[e]*Azerbaijan Medical University, Department of Cytology, Embryology, and Histology, Baku, AZ1022, Azerbaijan. E-mail: eldar.gasimov@amu.edu.az*

[f]*Azerbaijan Medical University, Department of Electron Microscopy of the Scientific Research Center, Baku, AZ1022, Azerbaijan. E-mail: fuad.rzayev@amu.edu.az*

© 2026 The Author(s). Published by the Royal Society of Chemistry

limitations related to poor penetration, instability, and insufficient therapeutic efficacy.[6–11] Among these approaches, nanoscale systems such as nanoemulsions, nanogels, and nanoemulgels have emerged as highly promising platforms due to their large surface area, tunable physicochemical properties, and favorable interactions with biological membranes.[12–15]

Nanoemulsions are kinetically stable colloidal dispersions typically characterized by droplet sizes below 1000 nm.[16] Their nanoscale dimensions facilitate improved dispersion of hydrophobic bioactive compounds and promote enhanced permeation across the skin barrier. However, despite these advantages, nanoemulsions may suffer from physicochemical instability during long-term storage, including droplet coalescence, creaming, or phase separation. To address these challenges, the integration of nanoemulsions into polymeric gel matrices has been widely explored, leading to the development of nanoemulgels. This hybrid delivery system combines the high solubilization capacity of nanoemulsions with the mechanical stability, improved rheology, and prolonged skin residence time provided by gel networks.[17,18]

Recent nanotechnological studies have demonstrated that the selection of an appropriate gel-forming polymer plays a critical role in determining the structural integrity, release behavior, and stability of nanoemulgel systems. Natural polysaccharides such as sodium alginate and pectin have gained particular attention due to their biocompatibility, biodegradability, low toxicity, and ability to form three-dimensional hydrogel networks through ion-mediated crosslinking mechanisms. These polymers enable effective entrapment of nanoemulsion droplets and allow controlled diffusion of encapsulated bioactive compounds, making them suitable candidates for advanced topical formulations.[19–22]

In parallel with nanotechnological advancements, increasing interest has been directed toward the incorporation of plant-derived bioactive compounds into nanoscale delivery systems. Phytochemical extracts rich in polyphenols, flavonoids, organic acids, and anthocyanins exhibit a broad spectrum of biological activities, including antioxidant, antimicrobial, anti-inflammatory, and regenerative effects.[23–26] *Hibiscus sabdariffa* L. flowers, in particular, have been extensively reported as a valuable source of bioactive constituents with demonstrated antibacterial, antifungal, and wound-healing potential. Nevertheless, the practical application of hibiscus extracts in topical formulations is often limited by their chemical instability and insufficient penetration through biological barriers.[27–29]

Hibiscus sabdariffa L. is a phytochemically rich medicinal plant containing several classes of bioactive constituents, particularly anthocyanins, phenolic acids, flavonoids, and organic acids. Among the major compounds reported in *H. sabdariffa* flowers are anthocyanins such as delphinidin-3-sambubioside and cyanidin-3-sambubioside, together with phenolic acids, flavonoid derivatives, and organic acids that collectively contribute to its reported antioxidant, antimicrobial, and anti-inflammatory activities. However, these phytochemical constituents, especially anthocyanins and other polyphenolic compounds, may be susceptible to degradation under unfavorable environmental conditions, including variations in pH, temperature, light, and oxygen exposure. Therefore, encapsulation of *H. sabdariffa* extract within a nanostructured delivery system represents a rational formulation strategy to improve the physicochemical protection of sensitive phytochemicals, enhance their dispersion within the formulation, and modulate their release from the polymeric matrix.[30,31]

Encapsulation of hibiscus flower extracts within nanotechnology-based delivery systems represents an effective strategy to overcome these limitations by protecting sensitive phytochemicals and enabling controlled release at the target site. Although several studies have reported nanoemulsion- or gel-based formulations containing plant extracts, systematic investigations focusing on nanoemulgel architectures that combine nanoscale dispersion, polymer-dependent matrix behavior, and long-term physicochemical stability remain limited.[32–34] In particular, comparative studies evaluating pectin- and sodium alginate-based nanoemulgels incorporating the same phytochemical extract under identical formulation and storage conditions are scarce in the literature.

From a translational and regulatory perspective, topical pharmaceutical formulations must comply with international stability and quality requirements to ensure safety, efficacy, and patient acceptability. Therefore, comprehensive physicochemical characterization and long-term stability evaluation in accordance with ICH and EMA principles are essential steps in the development of nanoemulgel-based drug delivery systems intended for practical use.[35,36]

We hypothesized that the distinct structural networks and molecular crosslinking behaviors of sodium alginate and pectin would differentially modulate the rheological attributes, colloidal stability, and diffusion kinetics of the encapsulated *Hibiscus sabdariffa* nanoemulsion, with the sodium alginate matrix providing superior polymeric organization for a more prolonged topical delivery. Accordingly, the present study aimed to design and comprehensively evaluate an advanced nanoemulgel delivery platform incorporating *Hibiscus sabdariffa* L. flower extract obtained *via* a high-speed extraction technique. In this approach, nanoemulsions were engineered and subsequently integrated into pectin- and sodium alginate-based gel matrices to systematically elucidate the impact of polymeric network structure on formulation performance. The developed nanoemulgels were thoroughly characterized with respect to their physicochemical attributes, morphological and rheological properties, *ex vivo* release behavior, and long-term stability under different storage and packaging conditions. Through this integrated nanotechnological and biopharmaceutical assessment, the study sought to identify a stable, effective, and translationally relevant nanoemulgel system suitable for topical application. The developed nanoemulgel systems were intended as preliminary formulation platforms for the topical delivery of *Hibiscus sabdariffa* L. flower extract. Accordingly, the present study focused on formulation development and comparative physicochemical, morphological, rheological, release, and stability characterization of pectin- and sodium alginate-based nanoemulgels. Direct dermal permeation or therapeutic efficacy was not investigated at this stage, and

© 2026 The Author(s). Published by the Royal Society of Chemistry

further studies using validated skin models will be required to establish their applicability for dermal delivery.

2. Experimental

2.1. Materials

Hibiscus flowers (*Hibiscus sabdariffa* L.) were used as the plant material in this study. The phytochemical extract employed in the formulation was previously developed and characterized by our research group using a high-speed extraction technique. Briefly, extraction was performed using a propylene glycol-ethanol solvent system (5 : 95, v/v), as reported in our earlier studies[37–39] The antibacterial and antifungal activities of the extract had been evaluated in these previous investigations; therefore, no additional antimicrobial testing of the extract itself was performed in the present study. The current work focused specifically on incorporation of the previously characterized extract into nanoemulsion and nanoemulgel systems and on evaluation of their formulation-related physicochemical and biopharmaceutical properties.

2.2. Preparation of nanoemulsions

Nanoemulsion formulations were prepared using the previously characterized phytochemical extract as the active component. Tween-20 (Sigma, Germany) and Span-80 (Merck, Germany) were employed as emulsifiers. Olive oil (Doğa İlaç, Türkiye) and linseed oil (Sigma, Germany) were used as oil phase and the emulsification process was carried out using a high-speed homogenizer (Stegler DG-360).

2.3. Particle size, polydispersity index, and zeta potential analysis

The resulting nanoemulsion formulations were characterized in terms of particle size, polydispersity index (PDI), and zeta potential using a Malvern Zetasizer Nano ZSP.[40,41] All measurements were performed in triplicate.

2.4. Preparation of nanoemulsion-based nanoemulgels

To improve the physical stability of the nanoemulsion system, nanoemulsion-based gels (nanoemulgels) were prepared using two different natural biopolymers with well-established rheological properties, namely sodium alginate (Alfa Aesar, Germany) and pectin (CPKelco, Denmark). Sodium alginate and pectin informations are below, in Table 1. For nanoemulgel preparation, the selected biopolymer was gradually incorporated into the optimized nanoemulsion under continuous stirring until a homogeneous gel matrix was obtained. The resulting formulations were allowed to equilibrate to ensure complete polymer hydration and uniform distribution of the nanoemulsion droplets within the gel network. The morphological characteristics of the prepared nanoemulgels were subsequently examined, and particle dimensions were evaluated at different magnification levels using appropriate imaging techniques. The structural integrity and functional properties of the nanoemulgels were further assessed using a combination of complementary analytical methods, as described in the following sections.[42,43]

Table 1 Sodium alginate and pectin informations

	Sodium alginate	Pectin
Catalog number	B25266	SK74013
Appearance	Pale brown powder	Cream to light tan
Molecular weight	NaN	—
Viscosity	Low viscosity	—
Assay	+95%	—
Loss on drying	10.4%	7.0
IR spectrum	Conforms to structure	—
Viscosity	100–200 cP (2% aqueous)	—
pH of 1% solution	—	4.5
Degree of methyl esterification	—	Typically 26%
Degree of methyl amidation		Typically 22%
Content of galacturonic acid residues	—	Min. 65%

The structural identity, functional groups, and physicochemical properties of the foundational polysaccharides (sodium alginate and pectin) were verified and characterized using Fourier Transform Infrared (FT-IR) spectroscopy, Energy-Dispersive X-ray (EDX) analysis, and rotational rheometry, ensuring the quality and integrity of the biopolymers prior to and after formulation.

2.5. pH measurement and rheology

The pH values of both blank and extract-loaded nanoemulgels were measured using a calibrated digital pH meter (InoLab pH Level 1). Measurements were performed separately for formulations based on sodium alginate and pectin to characterize the physicochemical properties of the formulations.[44–46]

Rheological properties, including viscosity, shear stress, and flow behavior, were analyzed using a rotational rheometer (Anton Paar Rheolab QC, Germany). Nanoemulgel samples were placed into the measuring container, and rheological measurements were performed at three different temperatures (20 °C, 40 °C, and 60 °C) under multiple measurement modes.

2.6. Morphological characterization

The morphological characteristics of the prepared nanoemulgels were examined using scanning electron microscopy (SEM) and transmission electron microscopy (TEM).[47–50] SEM analyses were performed using a Zeiss Sigma-300 instrument to evaluate surface morphology and particle size distribution. Prior to imaging, samples were mounted on aluminum stubs using carbon adhesive tape and sputter-coated with a thin layer of palladium for 800 seconds to ensure adequate conductivity. The coated samples were then placed in the SEM chamber and maintained under vacuum for 5 minutes before analysis. SEM images were acquired at an accelerating voltage of 5 kV (EHT = 5 kV), and particle diameters were measured at different

© 2026 The Author(s). Published by the Royal Society of Chemistry

magnification levels. TEM was carried out using a Hitachi HT7700 microscope to investigate the internal morphology and structural features of the nanoemulgel particles. TEM analysis provided detailed information on particle shape, size, and dispersion at the nanoscale, complementing the SEM observations.

2.7. Fourier transform infrared (FT-IR) spectroscopy

Fourier transform infrared (FT-IR) spectroscopy was employed to identify the characteristic functional groups of the nanoemulsion and nanoemulgel formulations and to assess potential intermolecular interactions among their components.[51] FT-IR spectra were recorded over the wavenumber range of 4000–400 cm^{-1} using a Shimadzu IR Spirit-T spectrophotometer.

2.8. Energy-dispersive X-ray (EDX) analysis

The elemental composition of the phytochemical extract-loaded nanoemulgels was analyzed using energy-dispersive X-ray (EDX) spectroscopy.[52–54] Measurements were performed with an EDX detector integrated into a scanning electron microscope (Zeiss Sigma-300). The relative weight and atomic percentages of the major constituent elements, including carbon (C), oxygen (O), sodium (Na), silicon (Si), chlorine (Cl), and calcium (Ca), were determined to confirm the elemental composition of the nanoemulgel matrices and the presence of inorganic components.

2.9. *Ex vivo* release studies

Ex vivo diffusion studies were conducted to comparatively evaluate the release of extract-derived bioactive compounds from the developed nanoemulgel formulations. Eggshell membrane was selected as a preliminary semi-permeable biological diffusion barrier because this model has previously been employed in diffusion/permeation studies of topical nanocarrier-loaded gels and related semisolid formulations. The membrane was used in the present study for comparative formulation assessment and was not intended to reproduce the barrier properties of human skin or to serve as a validated surrogate for dermal permeation.[55,56]

Prior to the experiment, the egg membrane was carefully separated and hydrated in phosphate buffer solution.[57,58] A fixed amount (2.0 g) of the nanoemulsion-based gel was placed in the donor compartment and brought into contact with the receptor compartment containing phosphate buffer (pH 7.4) through the egg membrane. The experiment was performed at 37 ± 1 °C for 24 h. Samples (5 mL) were withdrawn from the receptor medium at predetermined time intervals (every 30 min during the initial phase and subsequently at hourly intervals) and replaced with an equal volume of fresh buffer to maintain sink conditions. The collected samples were stored for subsequent spectrophotometric analysis to determine the cumulative release of bioactive compounds.

2.9.1. Quantification of the marker compound and method validation. The cumulative release of gallic acid, selected as the principal marker compound of *Hibiscus sabdariffa* extract, was quantified using a UV-Vis spectrophotometer (Shimadzu UV-1800, Japan) at λ_{max} = 271 nm. Gallic acid was previously identified as the predominant phenolic constituent of the extract (2870.95 ± 124.76 μg) by LC-MS/MS analysis in our earlier phytochemical study; therefore, release kinetics were calculated based on this marker compound.

The UV-Vis spectrophotometric analytical method was validated in compliance with International Council for Harmonisation (ICH Q2(R1)) guidelines:

2.9.1.1 Linearity and range. Calibration curves were constructed over a concentration range of 0.3125–5.000 μg mL^{-1} (312.5–5000 ng mL^{-1}). Linear regression analysis yielded the equation $y = 0.0542x + 0.0012$ with an excellent coefficient of determination ($R^2 = 0.9996$).

2.9.1.2 Specificity. Specificity was confirmed by comparing the UV spectra of pure gallic acid standard, blank formulation matrix, and dissolution media. No background spectral interference was detected at 271 nm.

2.9.1.3 Accuracy. Method accuracy was determined *via* recovery studies by spiking known concentrations of gallic acid at three levels ($n = 3$). The mean percentage recovery was within 98.45–101.20%.

2.9.1.4 Precision. Intra-day repeatability and inter-day intermediate precision were assessed ($n = 3$). All relative standard deviation (% RSD) values were well within the acceptable limit of <2.0% (intra-day % RSD < 1.45%; inter-day % RSD < 1.85%).

2.9.1.5 LOD and LOQ. The limit of detection (LOD) and limit of quantification (LOQ) were calculated based on the standard deviation of the response (σ) and the slope (S) of the calibration curve (LOD = $3.3\sigma/S$, LOQ = $10\sigma/S$). The LOD and LOQ were established as 0.00796 μg mL^{-1} (7.96 ng mL^{-1}) and 0.02413 μg mL^{-1} (24.13 ng mL^{-1}), respectively.

All measurements were performed in triplicate ($n = 3$), and results were expressed as mean pm standard deviation (SD). The complete analytical method validation parameters for the spectrophotometric quantification of gallic acid are summarized in Table 2.

2.10. Release kinetics analysis

Release kinetics were evaluated by fitting the *ex vivo* cumulative release data (%) of N1 and N5 to the Higuchi and Korsmeyer–Peppas models. Model parameters were estimated by linear regression and goodness-of-fit was assessed using the coefficient of determination (R^2).[59–61]

2.10.1. Higuchi model. The Higuchi model was applied to the early-to-mid release region (0–12 h) to describe diffusion-driven release from a matrix system:

$$Q_t = k_h\sqrt{t} + b$$

where Q_t is the cumulative release (%) at time t (h), k_H is the Higuchi release constant, and b is the intercept.

2.10.2. Korsmeyer–Peppas model. To gain insight into the release mechanism, the Korsmeyer–Peppas model was applied to the initial release phase ($M_t/M_\infty \leq 0.60$):

$$\frac{M_t}{M_\infty} = kt^n$$

© 2026 The Author(s). Published by the Royal Society of Chemistry

Table 2 Analytical method validation parameters for UV-Vis spectrophotometric quantification of gallic acid (ICH Q2(R1))

Parameter	Validation results/specifications
Instrument	Shimadzu UV-1800 UV-Vis spectrophotometer
Analytical wavelength (λ_{max})	271 nm
Linearity range	0.3125–5.000 μg mL^{-1} (312.5–5000 ng mL^{-1})
Regression equation	$y = 0.0542x + 0.0012$
Correlation coefficient (R^2)	0.9996
Specificity/selectivity	Specific (no spectral interference at 271 nm)
Accuracy (% recovery, $n = 3$)	98.45–101.20%
Intra-day precision (% RSD, $n = 3$)	<1.45%
Inter-day precision (% RSD, $n = 3$)	<1.85%
Limit of detection (LOD)	0.00796 μg mL^{-1} (7.96 ng mL^{-1})

The model was linearized as:

$$\ln\left(\frac{M_t}{M_\infty}\right) = \ln\ k + n\cdot\ln\ t$$

where M_t/M_∞ is the fraction released at time t, k is the kinetic constant, and n is the release exponent. Regression was performed using only data points satisfying $M_t/M_\infty \leq 0.60$.

2.11. Stability studies

The stability study was designed with reference to the general principles described in ICH Q1A(R2), while ICH Q1E was considered as a framework for the evaluation of stability data. The study was intended to comparatively assess the effects of storage temperature and packaging material on the physicochemical stability of the optimized nanoemulgel rather than to represent a formal regulatory stability program.[35,36] Samples were filled into hermetically sealed containers made of different packaging materials (glass and polymer) and stored under refrigerated conditions (4–8 °C) and controlled room temperature conditions (25 °C ± 2 °C/60% ± 5% RH). Long-term stability studies were conducted over a period of 12 months. At predetermined time points, the formulations were analyzed for critical physicochemical parameters, including pH, polydispersity index (PDI), and zeta potential, to assess their stability during storage.

All physicochemical measurements were performed in triplicate ($n = 3$), and the results are expressed as mean ± standard deviation (SD). Stability data were evaluated descriptively by monitoring changes in pH, zeta potential, polydispersity index, and active substance content over the 12 month storage period under each temperature and packaging condition.

3. Results and discussion

3.1. Formulation design and optimization of *Hibiscus* extract-loaded nanoemulsion and nanoemulgel systems

A nanoemulsion system was developed using a previously characterized *Hibiscus sabdariffa* L. extract obtained by a high-speed extraction method. To optimize formulation stability, eight different nanoemulsion compositions (Series 1–8) were systematically designed and prepared (Table 3). The formulations were developed by varying the oil phase (olive oil or flaxseed oil), surfactant/co-surfactant ratios (Tween-20 and Span-80), and ultrasonication conditions to identify a physically stable nanoemulsion system.

As summarized in Table 1, nanoemulsion formulations corresponding to Series 1–6 exhibited visible phase separation within 1–72 h, indicating insufficient kinetic stability. In Series 3, the incorporation of polyethylene glycol (PEG 400) failed to prevent phase separation, suggesting that the selected surfactant ratio and processing parameters were not optimal for long-term stability. Series 7 exhibited intermediate stability and remained physically stable for up to one month. However, among all tested formulations, Series 8 demonstrated superior stability, remaining visually homogeneous and free of phase separation for up to two months. Therefore, Series 8 was selected as the optimized nanoemulsion formulation and used for subsequent nanoemulgel preparation and further characterization studies.

Dynamic light scattering (DLS) analysis was performed to characterize the Hibiscus flower extract–loaded nanoemulsion in terms of droplet size, polydispersity index (PDI), and zeta potential. The nanoemulsion exhibited a mean droplet size of 419.70 ± 46.95 nm, indicating a submicron emulsion system with relatively narrow size variation. The PDI value was 0.48 ± 0.05, suggesting a moderately polydisperse but reproducible dispersion, which is commonly observed in phytochemical-loaded emulsions due to the complex composition of plant extracts.[62] The zeta potential was measured as −8.10 ± 0.74 mV, indicating a weak but consistent negative surface charge. Although this value reflects limited electrostatic stabilization, the nanoemulsion is primarily stabilized by steric effects provided by non-ionic surfactants at the oil–water interface. Overall, these results demonstrate that the extract-loaded nanoemulsion forms a physically acceptable and stable submicron dispersion, suitable for subsequent incorporation into a gel matrix for topical nanoemulgel formulation.[63]

To enhance the physical stability and topical applicability of the optimized nanoemulsion system, the nanoemulsion was incorporated into a gel matrix using a nanoemulsion-based gel (nanoemulgel) approach. Two natural polymers, sodium alginate and pectin, were selected as gelling agents owing to their biocompatibility and well-documented rheological properties. The composition of the prepared nanoemulgel formulations is summarized in Table 4. Based on the formulation optimization studies, the pectin-based and sodium alginate-based

© 2026 The Author(s). Published by the Royal Society of Chemistry

Table 3 Composition, processing conditions, and physical stability of the developed nanoemulsion formulations containing *Hibiscus sabdariffa* Extract

Component (g)	Series 1	Series 2	Series 3	Series 4	Series 5	Series 6	Series 7	Series 8
Olive oil	—	—	1.0	1.0	1.0	1.0	1.0	1.0
Linseed oil	1.0	1.0	—	—	—	—	—	—
Span 80	0.15	0.15	0.15	0.30	0.30	0.20	0.05	0.05
Tween 20	0.10	0.10	0.10	0.10	0.10	0.10	0.35	0.20
Hibiscus flower extract	0.5	0.5	0.5	0.5	0.5	0.5	0.5	0.5
Processing conditions	Homogenized for 1 min, followed by ultrasonication in three cycles of 20 s and two additional cycles of 1 min each	Homogenized for 1 min, followed by ultrasonication in three cycles of 20 s and one continuous cycle of 4 min	Homogenized for 1 min, followed by ultrasonication in sequential cycles of 10 s, 5 s, 5 s, 1 min, 40 s, and 1 min	Homogenized for 1 min, followed by ultrasonication in four consecutive cycles of 15 s	Homogenized for 1 min, the extract was subsequently added, and ultrasonication was applied in pulsed mode (10 s pulses)	Homogenized for 1 min, the extract was subsequently added, and ultrasonication was applied in pulsed mode (10 s pulses)	Homogenized for 1 min, the extract was subsequently added, and ultrasonication was applied in pulsed mode (10 s pulses)	Homogenized for 1 min, the extract was subsequently added, and ultrasonication was applied in pulsed mode (15 s pulses)
Stability	Phase separation after 1 h	Phase separation after 2 h	PEG 400 (150 mg) added; phase separation observed again	Phase separation after 24 h	Phase separation after 48 h	Phase separation after 72 h	Stable for 1 month	Stable for 2 months

nanoemulgel formulations, coded as N1 and N5, respectively, were identified as the most stable among the tested formulations. Accordingly, these optimized nanoemulgels were selected for further characterization and evaluation of their quality parameters.

3.2. pH and rheological characterization

The pH values of blank and extract-loaded nanoemulgel formulations based on sodium alginate and pectin were measured at room temperature using a calibrated digital pH meter (InoLab pH Level 1). The obtained results are summarized in Table 5.

The rheological behavior of the optimized nanoemulgel formulations N1 (pectin-based) and N5 (sodium alginate-based) was evaluated at different temperatures to assess their flow properties and thermal sensitivity. The rheological parameters are presented in Table 6, and the corresponding shear-dependent profiles are illustrated in Fig. 1.

The pectin-based nanoemulgel (N1) exhibited a well-structured gel network at lower temperatures, which gradually weakened as the temperature increased. Although an overall reduction in shear stress and viscosity was observed with increasing temperature, the gel structure was not completely disrupted, indicating that the formulation retained partial structural integrity even under elevated thermal conditions. This behavior suggests moderate thermal stability of the pectin-based system. Both the shear stress-shear rate and viscosity-shear rate profiles of N1 demonstrated a decrease in viscosity with increasing shear rate across all temperatures, confirming a pseudoplastic (shear-thinning) flow behavior. Such behavior is commonly associated with polymeric gel systems and can be attributed to the alignment and partial disentanglement of polymer chains under applied shear, resulting in reduced resistance to flow.[64]

In comparison, the sodium alginate-based nanoemulgel (N5) displayed a more thermally stable rheological profile. Although increases in temperature led to a reduction in viscosity and shear stress, the extent of structural weakening was less pronounced than that observed for the pectin-based formulation. This indicates that the alginate network maintained its structural integrity more effectively under thermal stress. Like N1, the N5 formulation also exhibited shear-thinning behavior at all tested temperatures, highlighting its pseudoplastic nature. The retention of this behavior across the entire temperature range indicates that the fundamental flow characteristics of the sodium alginate-based nanoemulgel were preserved despite thermal variations.

Overall, both formulations demonstrated temperature-dependent and pseudoplastic rheological behavior, which is advantageous for topical applications. High viscosity at low shear conditions supports formulation stability during storage, whereas viscosity reduction under shear facilitates ease of application and spreadability. Notably, the sodium alginate-based nanoemulgel (N5) exhibited comparatively greater resistance to temperature-induced structural changes, suggesting its

© 2026 The Author(s). Published by the Royal Society of Chemistry

Table 4 Composition of the developed nanoemulgel formulations based on different natural polymers

	Formulation code					
Component name (%)	N1	N2	N3	N4	N5	N6
Sodium alginate	—	3	—	0.5	1.5	—
Pectin	2	—	1	—	—	0.5
Nanoemulsion (*Hibiscus* extract)	15	15	15	15	15	15
Propylene glycol	5	5	5	5	5	5
Glycerin	2	2	2	2	2	2
Sodium benzoate	0.2	0.1	0.3	0.1	0.2	0.1
pH adjusting agent (NaOH/HCl)	As required (3.2–3.5)	As required (6.5–6.8)	As required (3.5–3.7)	As required (5.0–6.0)	As required (6.0–6.7)	As required (3.4–3.6)
Purified water	75.8	74.9	76.7	77.4	76.3	77.4

Table 5 pH values of nanoemulgel formulations based on sodium alginate and pectin[a]

Code	pH
N1-blank	3.93 ± 0.03
N1	3.60 ± 0.01
N5-blank	7.00 ± 0.10
N5	6.71 ± 0.01

[a] Calculations were performed using student's *t*-test ($P < 0.05$).

suitability for applications requiring enhanced rheological stability.

3.3 Morphological characterization of nanoemulgels

The surface morphology and internal structure of the optimized nanoemulgel formulations N1 (pectin-based) and N5 (sodium alginate-based) were investigated using scanning electron microscopy (SEM) and transmission electron microscopy (TEM). Representative images obtained at different scale bars are presented in Fig. 2.SEM images of the sodium alginate-based nanoemulgel (N5) revealed a compact and densely packed surface morphology at low magnification, with granular domains distributed across the matrix. As the scale bar decreased, the surface appeared increasingly homogeneous, indicating the formation of a tightly organized polymeric network. At the nanoscale, the matrix exhibited pronounced micro- and nanoscale surface features, indicating a comparatively compact organization of the sodium alginate-based matrix. In contrast, the pectin-based nanoemulgel (N1) exhibited a more open and heterogeneous surface morphology. SEM observations showed a porous and mesh-like structure with interconnected voids, which became more evident at higher magnifications. This morphology is characteristic of pectin-based gel systems and reflects a looser polymeric network formed around the nanoemulsion droplets. The presence of collapsed or partially dehydrated pores can be attributed to the sample preparation process required for SEM analysis.[65,66] TEM analysis further complemented the SEM observations by providing insight into the internal morphology of the nanoemulgel systems. TEM analysis complemented the SEM observations by revealing approximately spherical to oval nanoscale structures in both N1 and N5 formulations. These observations provide morphological evidence of nanoscale dispersed structures within the analyzed samples; however, electron microscopy alone does not allow their unequivocal identification as nanoemulsion droplets embedded within the polymeric gel matrix. Therefore, the TEM findings were interpreted primarily in terms of particle morphology rather than as direct evidence of nanoemulsion incorporation.[67]

Comparative morphological evaluation demonstrated distinct structural differences between the two nanoemulgel formulations. Comparative morphological evaluation revealed differences between the two nanoemulgel formulations. The sodium alginate-based formulation (N5) exhibited a comparatively denser and more compact surface morphology, whereas the pectin-based formulation (N1) showed a more porous and heterogeneous structure. These differences may be related to the intrinsic physicochemical characteristics of the respective polymer matrices. TEM images of both formulations additionally showed approximately spherical to oval nanoscale structures. Overall, the electron microscopy findings demonstrate polymer-dependent morphological differences between N1 and N5, while avoiding definitive attribution of the observed nanoscale structures to nanoemulsion droplets (Fig. 3).

3.4. FT-IR analysis and intermolecular interactions

FT-IR spectroscopy was used to compare the spectral characteristics of the blank and extract-loaded pectin-based (N1) and sodium alginate-based (N5) nanoemulgels. The corresponding spectra are presented in Fig. 4. In both polymer systems, broad O–H stretching bands were observed in the 3200–3600 cm^{-1} region. Following incorporation of the extract, slight differences in band shape and intensity were observed. These changes may be consistent with alterations in the local hydrogen-bonding environment; however, they cannot be considered definitive evidence of specific molecular interactions.

In the sodium alginate-based formulation, minor spectral differences were observed in regions associated with carboxylate groups, whereas the pectin-based formulation showed slight variations in the carbonyl-associated region. These

© 2026 The Author(s). Published by the Royal Society of Chemistry

Table 6 Rheological parameters of nanoemulgel formulations (N1 and N5) at different temperatures

		20 °C		40 °C		60 °C	
No.	Shear speed, γ (s^{-1})	Dynamic viscosity, η (mPa s)	Shear stress, τ (Pa)	Dynamic viscosity, η (mPa s)	Shear stress, τ (Pa(	Dynamic viscosity, η (mPa s(	Shear stress, τ (Pa)
N1 (pectin-based nanoemulgel)							
1	64.44	706.3	45.51	333.4	21.49	167.6	10.80
2	128.87	633.8	81.68	313.2	40.36	164.5	21.20
3	193.31	582.0	112.50	298.0	57.60	160.9	31.10
4	257.75	541.1	139.46	285.9	73.68	157.9	40.70
5	322.19	508.7	163.88	275.5	88.75	155.6	50.15
6	386.62	481.8	186.27	265.9	102.79	153.6	59.39
7	451.06	458.4	206.78	257.3	116.04	151.1	68.16
8	515.5	438.2	225.89	249.9	128.81	149.2	76.92
9	579.94	420.6	243.94	243.3	141.10	147.5	85.52
10	644.37	405.6	261.34	238.0	153.37	146.6	94.45
N5 (sodium alginate-based nanoemulgel)							
1	64.44	583.3	37.58	308.9	19.90	181.0	11.66
2	128.87	537.9	69.32	293.8	37.86	175.6	22.63
3	193.31	503.4	97.31	281.7	54.45	170.0	32.86
4	257.75	475.0	122.42	271.3	69.92	165.7	42.70
5	322.19	451.3	145.40	262.5	84.58	162.3	52.30
6	386.62	431.8	166.93	254.6	98.45	159.5	61.68
7	451.06	414.71	187.05	247.6	111.69	157.0	70.82
8	515.5	399.3	205.85	241.4	124.44	154.6	79.71
9	579.94	385.6	223.65	235.9	136.79	152.4	88.38
10	644.37	373.7	240.79	231.5	149.15	150.2	96.80

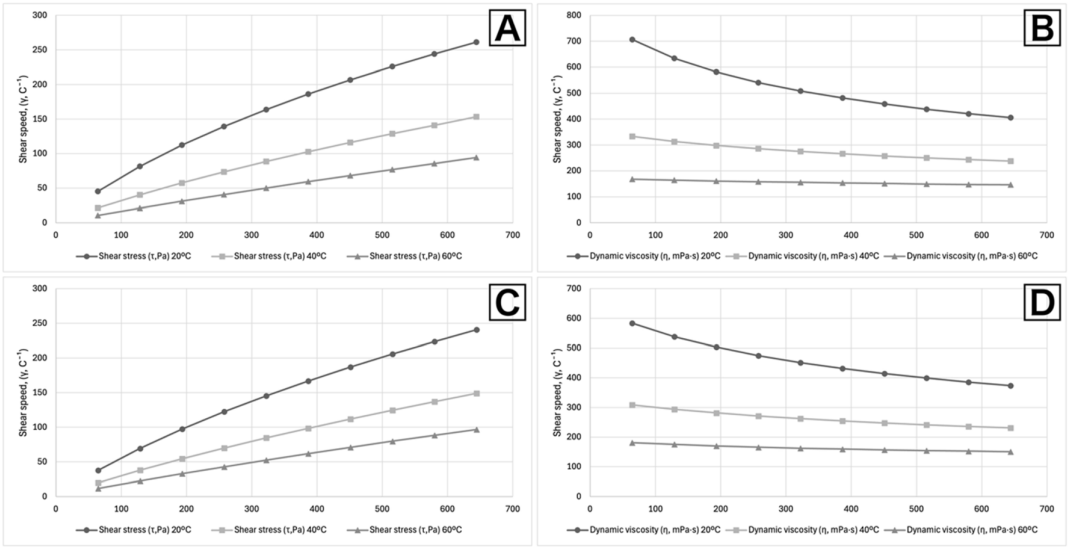

Fig. 1 Shear-dependent rheological behavior of optimized nanoemulgel formulations (N1 and N5). (A) Shear stress as a function of shear rate for the pectin-based nanoemulgel (N1). (B) Dynamic viscosity as a function of shear rate for the pectin-based nanoemulgel (N1). (C) Shear stress as a function of shear rate for the sodium alginate-based nanoemulgel (N5). (D) Dynamic viscosity as a function of shear rate for the sodium alginate-based nanoemulgel (N5).

changes may reflect non-covalent interactions among formulation components, although assignment of a specific interaction mechanism based solely on FT-IR spectra would be speculative. The major polysaccharide-associated bands remained detectable in both blank and extract-loaded formulations, and no marked new absorption bands were observed. Overall, the FT-IR findings indicate that extract loading produced only limited spectral changes in the polymer-based formulations and are consistent with predominantly physical associations among formulation components.[68,69]

© 2026 The Author(s). Published by the Royal Society of Chemistry

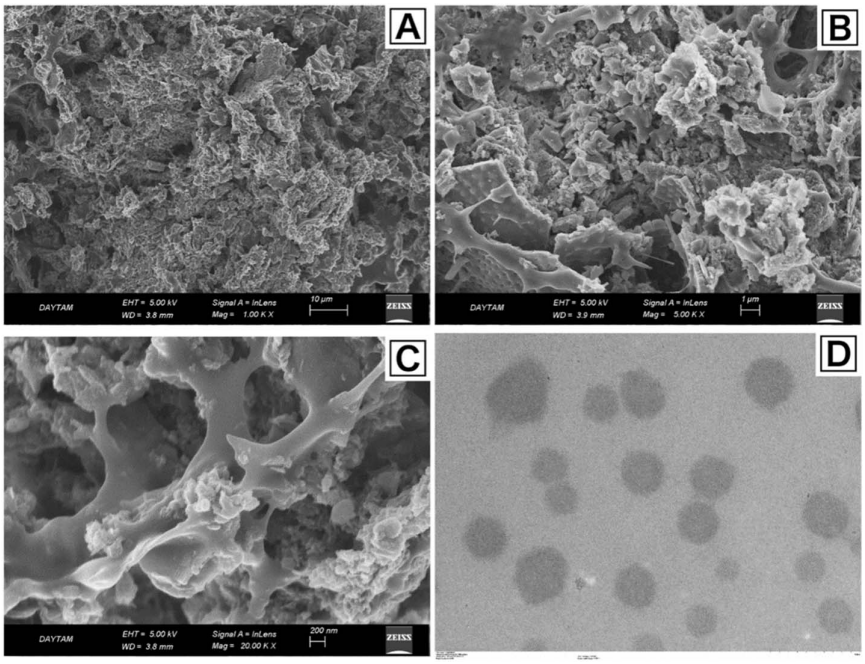

Fig. 2 Representative scanning electron microscopy (SEM) and transmission electron microscopy (TEM) images of the optimized pectin-based nanoemulgel formulation (N1). SEM images obtained at scale bars of (A) 10 μm, (B) 1 μm, and (C) 200 nm illustrate the relatively porous and heterogeneous surface morphology of the pectin-based matrix. The corresponding TEM image (D) shows approximately spherical nanoscale structures associated with the dispersed nanoemulsion phase.

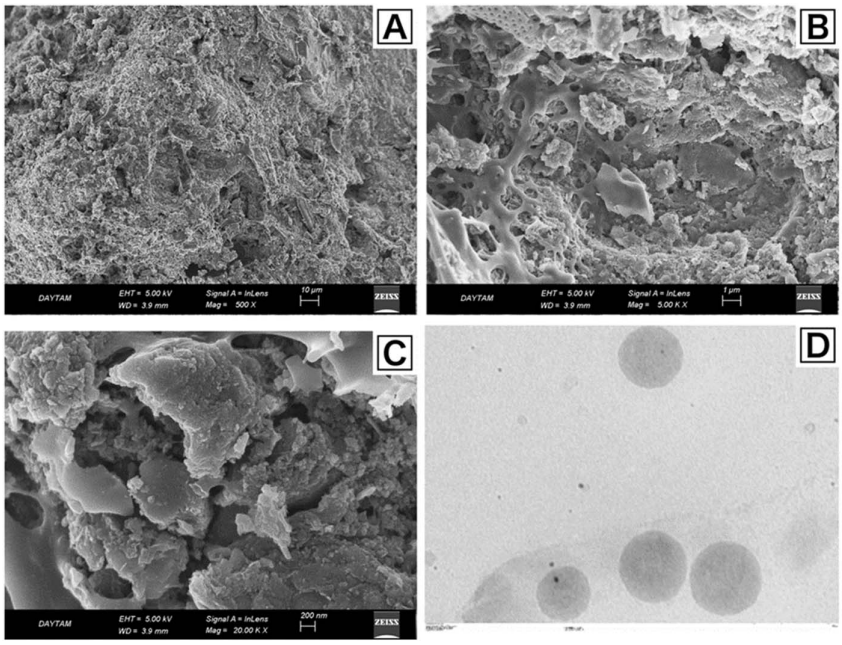

Fig. 3 Representative scanning electron microscopy (SEM) and transmission electron microscopy (TEM) images of the optimized sodium alginate-based nanoemulgel formulation (N5). SEM images obtained at scale bars of (A) 10 μm, (B) 1 μm, and (C) 200 nm show a comparatively denser and more compact surface morphology of the sodium alginate-based matrix. The corresponding TEM image (D) shows approximately spherical nanoscale structures associated with the dispersed nanoemulsion phase.

© 2026 The Author(s). Published by the Royal Society of Chemistry

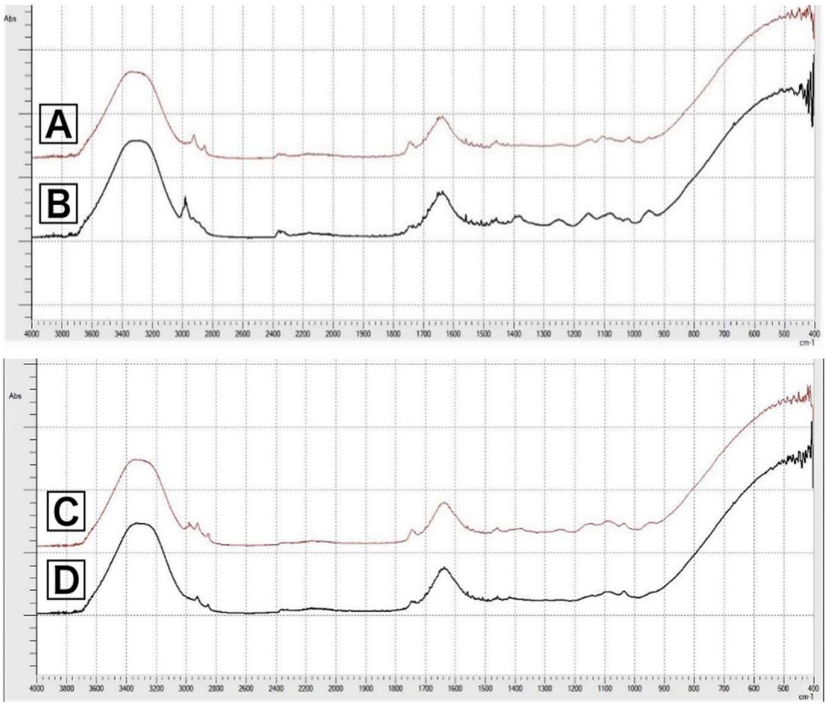

Fig. 4 Fourier transform infrared spectroscopy (FT-IR) spectra of the optimized nanoemulgel formulations. The FT-IR spectrum of the blank pectin-based nanoemulgel (N1-Blank) is shown in (A), while the extract-loaded pectin-based nanoemulgel (N1) is presented in (B). The FT-IR spectrum of the blank sodium alginate-based nanoemulgel (N5-Blank) is shown in (C), and the extract-loaded sodium alginate-based nanoemulgel (N5) is presented in (D).

3.5. Elemental composition analysis by EDX

Energy-dispersive X-ray (EDX) spectroscopy was used to obtain semi-quantitative elemental profiles of the extract-loaded pectin-based (N1) and sodium alginate-based (N5) nanoemulgels. The corresponding spectra and elemental compositions are presented in Fig. 5 and Table 7. Carbon and oxygen were the predominant detected elements in both formulations, consistent with the organic and polysaccharide-rich composition of the systems. Sodium was detected in both formulations and was present at a higher level in N5, which is consistent with the presence of sodium alginate in this formulation.

Minor amounts of Si and Ca were detected in N1, whereas Si, P, S, Cl, and Ca were detected at low levels in N5. Because EDX provides elemental rather than molecular information, the specific origin of these minor elements cannot be assigned unequivocally to individual formulation components or to the plant extract. Accordingly, these findings are interpreted descriptively rather than as evidence of specific molecular interactions or formulation incorporation. Overall, the EDX analysis provides a comparative elemental profile of the two nanoemulgel formulations, with the principal difference being the higher sodium contribution observed for the sodium alginate-based N5 formulation.

3.6 *Ex vivo* release behavior of biologically active compounds

The *ex vivo* diffusion study was performed to evaluate the release behavior of extract-derived bioactive compounds from the optimized pectin-based (N1) and sodium alginate-based (N5) nanoemulgel formulations using an egg membrane model. The cumulative release profiles over 24 hours are illustrated in Fig. 6. For the pectin-based nanoemulgel (N1), the release curve exhibits a characteristic diffusion-controlled profile with multiple stages. During the initial period (≈0–2 h), the cumulative release remained very low (≈0–5%), indicating the absence of an immediate burst effect. This behavior suggests that the majority of extract-derived bioactive compounds were effectively immobilized within the polymeric network and not freely available at the gel surface. Between approximately 2 and 6 hours, a gradual increase in cumulative release (≈10–45%) was observed, corresponding to the onset of diffusion-driven transport through the hydrated pectin matrix. In this region, the slope of the release curve increased progressively, indicating time-dependent diffusion governed by the polymer network structure and swelling behavior. At later time points (≈6–12 h), the release rate continued to increase, reaching approximately 90–95% cumulative release. This prolonged release phase reflects diffusion through a partially relaxed gel network, where molecular transport becomes increasingly facilitated as hydration progresses. Over the full experimental duration (≈20–24 h), cumulative release approached completion (≈99%), confirming the extended-release capability of the pectin-based system under *ex vivo* conditions.

The sodium alginate-based nanoemulgel (N5) demonstrated a comparatively more sustained release profile. During the early

© 2026 The Author(s). Published by the Royal Society of Chemistry

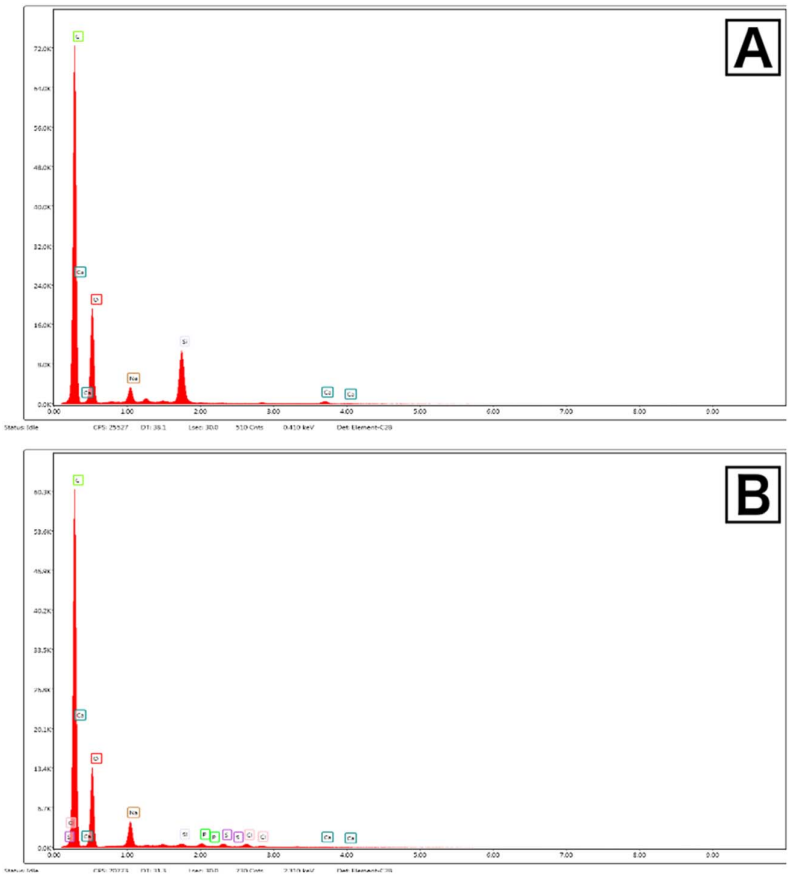

Fig. 5 Energy-dispersive X-ray (EDX) spectroscopy spectra of the optimized nanoemulgel formulations. The EDX spectrum of the extract-loaded pectin-based nanoemulgel (N1) is shown in (A), while the EDX spectrum of the extract-loaded sodium alginate-based nanoemulgel (N5) is shown in (B).

Table 7 Elemental composition of extract-loaded nanoemulgel formulations based on pectin (N1) and sodium alginate N5)

	Element	Weight %	Atomic %
N1	C	68.0	76.4
	O	22.4	18.9
	Na	2.7	1.6
	Si	6.1	2.9
	Ca	0.8	0.3
N5	C	70.2	77.6
	O	22.1	18.3
	Na	5.2	3.0
	Si	0.4	0.2
	P	0.6	0.2
	S	0.6	0.2
	Cl	0.7	0.3
	Ca	0.3	0.1

phase (≈0–1 h), no detectable release was observed, followed by a limited initial diffusion stage between approximately 1 and 3 hours (≈5–15%). The reduced initial slope of the release curve indicates stronger retention of BAC within the alginate network and minimal surface-associated diffusion. In the intermediate phase (≈4–9 h), cumulative release increased steadily (≈20–65%), consistent with diffusion-controlled transport through a denser polymeric matrix. Compared with the pectin-based formulation, the slope of the release curve for N5 was lower, indicating slower diffusion kinetics. At later stages (≈10–12 h), cumulative release reached approximately 85–90%, followed by a gradual approach to near-complete release (≈99%) by 20–24 hours.

Overall, both nanoemulgel formulations exhibited controlled and prolonged BAC release profiles characterized by limited initial diffusion and time-dependent transport through polymeric networks. The differences observed between N1 and N5 highlight the influence of polymer structure and network density on diffusion kinetics. While the pectin-based nanoemulgel showed relatively faster release, the sodium alginate-based formulation provided a more sustained and gradual release behavior.

Considering both release characteristics and formulation properties, the sodium alginate-based nanoemulgel demonstrated a more favorable profile for prolonged topical delivery. In addition, the pH of the pectin-based formulation was below the physiological skin pH range, which may restrict its practical

© 2026 The Author(s). Published by the Royal Society of Chemistry

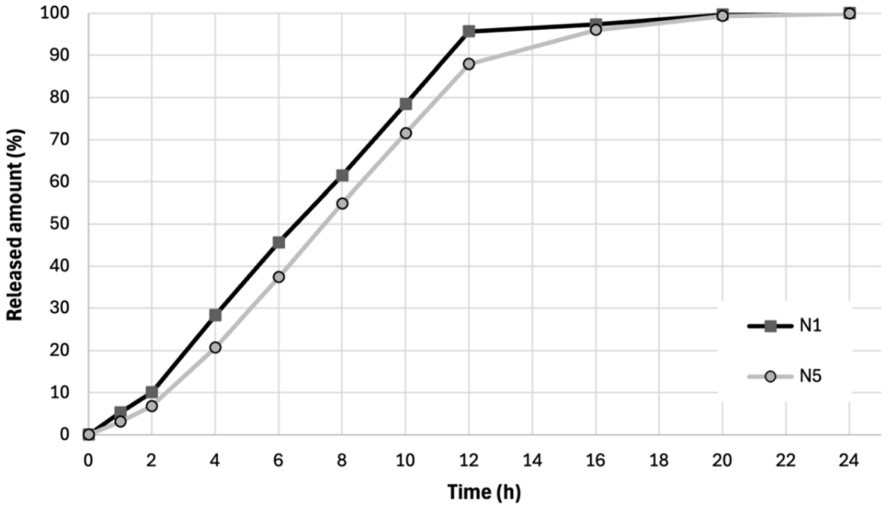

Fig. 6 *Ex vivo* cumulative release profiles of extract-derived bioactive compounds from pectin- and sodium alginate-based nanoemulgel formulations (N1 and N5).

applicability. In contrast, the sodium alginate-based formulation exhibited a pH closer to neutrality together with a comparatively more gradual release profile, and was therefore selected for further formulation and stability evaluation. These physicochemical findings should not be interpreted as direct evidence of skin compatibility, which requires dedicated biological and dermal studies.

3.7. Release kinetics

Both formulations exhibited sustained release over 24 h, approaching complete release at the end of the test period (N1: 99.95%, N5: 99.92%). For mechanistic interpretation, kinetic modeling was performed. The calculated kinetic parameters and correlation coefficients obtained from both models are summarized in Table 8.[59–61,70]

3.7.1. Higuchi fitting (0–12 h). Cumulative release plotted against $\sqrt{t}$ showed an apparent linear relationship for both formulations during the early-to-mid release phase (0–12 h), indicating that diffusion may contribute to the observed release behavior. However, considering the moderate coefficients of determination, the Higuchi fit was not interpreted as definitive evidence of a purely diffusion-controlled release mechanism. The estimated Higuchi constants indicated slightly faster release from N1 compared with N5, consistent with the more sustained profile of N5 (Table 6).

3.7.2. Korsmeyer–Peppas fitting (≤60% release). Korsmeyer–Peppas analysis was conducted using the initial fraction released ($M_t/M_\infty \leq 0.60$). N1 was modeled using 1–6 h data (up to 45.6%), whereas N5 included 1–8 h data (up to 54.8%). Both formulations yielded high R^2 values, indicating an excellent empirical fit in the early phase. Both formulations yielded high R^2 values, indicating a good empirical fit within the initial release region. The obtained n values were >1; however, because the Korsmeyer–Peppas model is empirical and its exponent is dependent on system geometry and experimental conditions, these values were interpreted cautiously and were not considered definitive evidence of a specific transport mechanism. This consideration is particularly relevant to the present system, in which release from a semisolid polymeric matrix was evaluated across an egg-membrane diffusion barrier (Table 8).[71–73]

3.8. Stability evaluation of nanoemulgels

The stability of the Hibiscus extract-loaded sodium alginate-based nanoemulgel (N5) was evaluated under long-term storage conditions using a natural aging approach in accordance with ICH Q1A(R2) principles. The formulation was stored

Table 8 Release kinetic parameters of nanoemulgel formulations (N1 and N5) fitted to Higuchi (0–12 h) and Korsmeyer–Peppas ($M_t/M_\infty \leq 0.60$) models

Model	Parameter	N1	N5	Data
Higuchi $Q_t = k_h\sqrt{t} + b$	k_h	28.65	26.32	0–12 h
	b	−17.86	−18.42	0–12 h
	R^2	0.897	0.866	0–12 h
Korsmeyer–Peppas	n	1.231	1.413	N1: 1–6 h; N5: 1–8 h
$\frac{M_t}{M_\infty} = kt^n$	k	0.0493	0.0289	$M_t/M_\infty \leq 0.60$
	R^2	0.991	0.996	$M_t/M_\infty \leq 0.60$

© 2026 The Author(s). Published by the Royal Society of Chemistry

Table 9 Long-term stability results of Hibiscus extract-loaded sodium alginate-based nanoemulgel (N5) stored under different temperature and packaging conditions[a]

Months	pH	Zeta (mV)	PDI	Active substance
Stability results of hibiscus extract–loaded sodium alginate-based nanoemulgel (N5) stored in glass vials at 4–8 °C				
0	6.71 ± 0.01	−28 ± 0.5	0.22 ± 0.01	100% ± 0.5
1	6.71 ± 0.01	−28 ± 0.5	0.22 ± 0.01	100% ± 0.5
3	6.71 ± 0.02	−28 ± 0.6	0.22 ± 0.01	100% ± 0.5
6	6.71 ± 0.01	−28 ± 0.6	0.22 ± 0.01	100% ± 0.7
9	6.70 ± 0.02	−27 ± 0.7	0.23 ± 0.02	99% ± 0.8
12	6.69 ± 0.02	−26 ± 0.8	0.24 ± 0.02	98% ± 0.9
Stability results of hibiscus extract-loaded sodium alginate-based nanoemulgel (N5) stored in glass vials at 22–25 °C				
0	6.71 ± 0.01	−28 ± 0.6	0.22 ± 0.01	100% ± 0.4
1	6.70 ± 0.02	−27 ± 0.7	0.23 ± 0.01	99% ± 0.70
3	6.69 ± 0.02	−26 ± 0.8	0.25 ± 0.02	97% ± 0.80
6	6.68 ± 0.03	−25 ± 0.9	0.28 ± 0.02	95% ± 1.0
9	6.66 ± 0.03	−24 ± 1.1	0.30 ± 0.03	93% ± 1.2
12	6.64 ± 0.04	−22 ± 1.3	0.34 ± 0.03	90% ± 1.4
Stability results of hibiscus extract-loaded sodium alginate-based nanoemulgel (N5) stored in plastic vials at 4–8 °C				
0	6.71 ± 0.02	−28 ± 0.7	0.22 ± 0.01	100% ± 0.6
1	6.68 ± 0.02	−25 ± 1.0	0.28 ± 0.02	97% ± 0.8
3	6.65 ± 0.03	−20 ± 1.1	0.40 ± 0.03	92% ± 1.1
6	6.60 ± 0.04	−16 ± 1.4	0.55 ± 0.04	85% ± 1.4
9	6.55 ± 0.05	−14 ± 1.7	0.70 ± 0.05	75% ± 1.9
12	6.50 ± 0.06	−12 ± 2.0	0.85 ± 0.06	65% ± 2.2
Stability results of hibiscus extract-loaded sodium alginate-based nanoemulgel (N5) stored in plastic vials at 22–25 °C				
0	6.71 ± 0.01	−28 ± 0.6	0.22 ± 0.01	100% ± 0.5
1	6.65 ± 0.03	−22 ± 1.1	0.35 ± 0.02	94% ± 1.2
3	5.58 ± 0.05	−18 ± 1.4	0.55 ± 0.04	88% ± 1.6
6	5.52 ± 0.07	−14 ± 1.8	0.70 ± 0.05	80% ± 2.1
9	4.45 ± 0.10	−12 ± 2.2	0.85 ± 0.70	70% ± 2.8
12	3.40 ± 0.15	−10 ± 2.8	1.00 ± 0.12	58% ± 3.5

[a] A one-way ANOVA test was applied to calculate the mean value (mean ± SD) for $n = 3$ trials ($p < 0.05$).

in different container types (glass and plastic vials) at refrigerated (4–8 °C) and room temperature (22–25 °C) conditions, and changes in pH, zeta potential, polydispersity index (PDI), and active substance content were monitored over a 12 month period. A comprehensive overview of the stability evaluation parameters is provided in Table 9. Following formulation optimization, the nanoemulgel formulation coded as N5 was identified as the optimal system and therefore selected as the sole candidate for detailed long-term stability evaluation.

When stored in glass vials at 4–8 °C, the nanoemulgel exhibited excellent physicochemical stability. Only minimal changes in pH were observed over 12 months, while zeta potential values remained within a range indicative of preserved colloidal integrity. The PDI showed negligible variation, confirming maintenance of particle size homogeneity, and the active substance content remained above 98% at the end of the study period. These findings demonstrate that the formulation fulfills the criteria for long-term stability under refrigerated conditions.

In contrast, storage in glass vials at 22–25 °C resulted in gradual deterioration of physicochemical properties. Although pH changes remained moderate, a progressive decrease in zeta potential and an increase in PDI were observed, indicating partial loss of colloidal stability. Additionally, a noticeable reduction in active substance content was detected by the end of the 12 month period. According to ICH stability expectations, these changes suggest that room temperature storage in glass vials is less suitable for long-term preservation of the nanoemulgel.

Stability studies conducted in plastic vials revealed a pronounced negative effect of packaging material on formulation integrity. Even under refrigerated conditions, significant reductions in zeta potential, marked increases in PDI, and substantial losses of active substance were observed over time. These effects were further exacerbated at 22–25 °C, where sharp pH decreases, severe colloidal destabilization, and extensive active substance loss occurred. The results clearly indicate incompatibility between the nanoemulgel formulation and plastic packaging, likely due to adsorption, diffusion, or migration phenomena.

Overall, comparative stability assessment demonstrates that the Hibiscus extract-loaded sodium alginate-based nanoemulgel exhibits optimal long-term stability when stored in glass vials under refrigerated conditions (4–8 °C). These findings are consistent with ICH and EMA expectations and support

© 2026 The Author(s). Published by the Royal Society of Chemistry

the recommended storage conditions for the developed nanoemulgel formulation.

4. Conclusion

In the present study, a nanotechnology-driven nanoemulgel platform incorporating *Hibiscus sabdariffa* L. flower extract was successfully developed and comprehensively characterized. The optimized nanoemulsion exhibited submicron droplet size, moderate polydispersity, and consistent negative surface charge, confirming its suitability for topical formulation *via* steric stabilization mechanisms. Incorporation of the nanoemulsion into biopolymer-based gel matrices significantly enhanced physicochemical stability, rheological behavior, and release control. Comparative evaluation demonstrated that polymer selection critically influenced nanoemulgel performance. While both pectin- and sodium alginate-based systems formed structurally integrated nanoemulgels, the sodium alginate-based formulation (N5) exhibited superior thermal resistance, sustained release behavior, and pH compatibility with the skin. Release kinetic analysis provided an empirical description of the release profiles and suggested a contribution of diffusion, although no definitive transport mechanism was assigned based solely on the applied mathematical models. Morphological and spectroscopic analyses revealed polymer-dependent structural characteristics and limited spectral changes following extract incorporation. Morphological analyses revealed distinct polymer-dependent structural features in the optimized formulations. Importantly, long-term stability studies performed in compliance with ICH and EMA principles identified glass packaging under refrigerated conditions (4–8 °C) as the optimal storage environment, ensuring preservation of colloidal stability and active substance content for at least 12 months. In contrast, plastic packaging and room temperature storage were associated with progressive physicochemical degradation. Taken together, these findings support the sodium alginate–based nanoemulgel as a promising formulation candidate for further development toward topical delivery of *Hibiscus sabdariffa* extract. However, the egg membrane study should be regarded as a preliminary comparative diffusion assessment, and further studies using validated *ex vivo* human or animal skin models, together with appropriate biological evaluations, are required to establish dermal permeation, safety, and therapeutic performance.

Author contributions

Bahruz S. Mammadov: conceptualization, resources, writing – original draft, writing – review and editing. Sevil J. Mehraliyeva: supervision, project administration, conceptualization, writing – original draft. Rukiye Sevinc Özakar: methodology, investigation, formal analysis, visualization, writing – original draft, writing – review and editing. Emrah Özakar: methodology, investigation, visualization, formal analysis, writing – original draft, writing – review and editing. Yasin Bayır: methodology, investigation, visualization, formal analysis, writing – original draft, writing – review and editing. A. Alper Öztürk: methodology, investigation, formal analysis, writing – original draft, writing – review and editing. Eldar Qasimov: visualization, writing – original draft, writing – review and editing. Fuad Rzayev: visualization, writing – original draft, writing – review and editing.

Conflicts of interest

The authors declare no competing interests. The study was conducted without any commercial or financial relationships that could be interpreted as potential conflicts of interest.

Data availability

The data supporting the findings of this study, including the physicochemical characterization, rheological measurements, *in vitro* release profiles, stability study results, and spectroscopic and microscopic analyses (FT-IR, EDX, SEM, and TEM), are presented within this article.

Acknowledgements

The authors gratefully acknowledge the Scientific Research Center of Azerbaijan Medical University (AMU) for providing laboratory facilities and technical support.

References

1 Ş. Şahin, E. Kaya-Tilki, M. Baysal and A. A. Öztürk, *Sci. Rep.*, 2025, **15**, 36194, DOI: 10.1038/s41598-025-20012-x.
2 B. Solak, P. Soyer, E. K. Tilki and A. A. Öztürk, *J. Drug Deliv. Sci. Technol.*, 2025, 106721, DOI: 10.1016/j.jddst.2025.106721.
3 T. Çevikelli, U. M. Güven and A. A. Öztürk, *FABAD J. Pharm. Sci.*, 2024, **49**, 111–128, DOI: 10.55262/fabadeczacilik.1359138.
4 E. Kaya-Tilki, A. A. Öztürk, S. Engür-Öztürk and M. Dikmen, *Sci. Rep.*, 2024, **14**, 19837, DOI: 10.1038/s41598-024-70791-y.
5 B. Kurban, T. Tuncel, Ş. Görgülü, F. Kar, A. Öztürk and T. Özek, *J. Cell. Mol. Med.*, 2023, **27**, 1887–1899, DOI: 10.1111/jcmm.17801.
6 A. Raghav, S. Negi, V. Masiwal, F. Mascarenhas-Melo and A. Lohani, *Nanodermatology*, 2026, 3–22, DOI: 10.1016/B978-0-443-36326-9.00023-X.
7 M. D. Ansari, H. Majid, S. Mahmood, Z. M. Sofian, A. Husain, Y. Sultana and F. Shakeel, *Asian Pac. J. Trop. Biomed.*, 2026, **16**, 1–23, DOI: 10.4103/apjtb.apjtb_491_25.
8 N. Taba, P. Kumar, K. Kalra and M. Yashpal, *Nanodermatology*, 2026, 409–436, DOI: 10.1016/B978-0-443-36326-9.00020-4.
9 W. Lu, J. Cao, Y. Lv, M. Li, Y. Tang and Y. Feng, *AAPS PharmSciTech*, 2025, **27**, 21, DOI: 10.1208/s12249-025-03244-y.
10 Z. Yan, S. Zhang, G. Wu, Y. Kang, C. Fu, Z. Wang, G. Wang, L. Tang and W. Wang, *Pharmaceutics*, 2026, **18**, 63, DOI: 10.3390/pharmaceutics18010063.

© 2026 The Author(s). Published by the Royal Society of Chemistry

11 A. A. Öztürk, Y. Uzun and F. Z. Saltan, *J. Drug Deliv. Sci. Technol.*, 2025, **113**, 107352, DOI: 10.1016/j.jddst.2025.107352.
12 A. Tošić, D. Randjelović, B. Ivković, A. Gledović, T. Stanković, J. Đoković, V. Papadimitriou, T. Ilić, S. D. Savić and I. Pantelić, *Pharmaceutics*, 2025, **17**, 1532, DOI: 10.3390/pharmaceutics17121532.
13 S. K. Gupta and N. Chaubey, *Int. J. Pharm. Investig.*, 2025, **15**, 377–387, DOI: 10.5530/ijpi.20251793.
14 A. Ansari, M. Verma and S. Majhi, *Micro Nanosyst.*, 2025, **17**, 12–26, DOI: 10.2174/0118764029316500240904074317.
15 U. Abbasi, M. Z. Khan, M. Fatima, G. Gupta, N. Molugulu, A. Sahebkar, M. A. S. Abourehab and P. Kesharwani, *J. Drug Target.*, 2025, **33**, 1343–1365, DOI: 10.1080/1061186X.2025.2497368.
16 Y. N. Ashagrie, M. G. Tadesse, R. K. Bachheti, G. Nijhawan, S. Tyagi and A. Bachheti, *Sci. Rep.*, 2025, **15**, 14598, DOI: 10.1038/s41598-025-87732-y.
17 B. K. Yadav, R. Patel, B. Prajapati and G. Patel, *Curr. Pharm. Biotechnol.*, 2025, **26**, 1906–1920, DOI: 10.2174/0113892010312939240704141630.
18 S. S. Nedel, S. da Silva Gündel, M. L. Machado, F. B. O. Baptista, B. Klein, F. Candido, F. R. Favarin, K. W. Krawczak, A. Gündel, R. Wagner, F. A. A. Soares, C. R. Boeck and A. F. Ourique, *J. Drug Deliv. Sci. Technol.*, 2026, **115**, 107652, DOI: 10.1016/j.jddst.2025.107652.
19 J. Cao, B. Wu, P. Yuan, Y. Liu and C. Hu, *Gels*, 2025, **11**, 758, DOI: 10.3390/gels11090758.
20 M. Akbar, A. Yaqoob, A. Ahmad, R. Luque, *Sodium Alginate-Based Nanomaterials for Wastewater Treatment*, Elsevier, 2023, pp. 1–17, DOI: 10.1016/B978-0-12-823551-5.00012-4.
21 S. Popov, N. Paderin, D. Khramova, E. Kvashninova, A. Melekhin and F. Vityazev, *Mar. Drugs*, 2022, **20**, 94, DOI: 10.3390/md20020094.
22 N. S. Said, I. F. Olawuyi and W. Y. Lee, *Gels*, 2023, **9**, 732, DOI: 10.3390/gels9090732.
23 A. M. Saad, D. M. Mohammed, S. S. Alkafaas, S. Ghosh, S. H. Negm, H. M. Salem, M. A. Fahmy, H. E. Semary, E. H. Ibrahim, S. F. AbuQamar, K. A. El-Tarabily and M. T. El-Saadony, *Front. Immunol.*, 2025, **16**, 1653378, DOI: 10.3389/fimmu.2025.1653378.
24 S. Sun, Y. Yu, Y. Jo, J. H. Han, Y. Xue, M. Cho, S.-J. Bae, D. Ryu, W. Park, K.-T. Ha and S. Zhuang, *Front. Pharmacol*, 2025, **16**, 1615338, DOI: 10.3389/fphar.2025.1615338.
25 H. Xing, G. Li, C. Qi, M. Zhang, N. Ding and X. Zhang, *Int. J. Nanomedicine*, 2025, **20**, 12715–12731, DOI: 10.2147/IJN.S547550.
26 M. D. Langellotto, G. Rassu, C. Serri, S. Demartis, P. Giunchedi and E. Gavini, *Drug Deliv. Transl. Res.*, 2025, **15**, 831–845, DOI: 10.1007/s13346-024-01698-4.
27 L. Mouhi, A. Belkadi, A. Amrane, A. Toubane, H. Guedjali and L. Chouial, *J. Pharm. Innov.*, 2026, **21**, 66, DOI: 10.1007/s12247-025-10287-y.
28 A. C. S. Nogueira da Cruz, M. J. T. A. Madruga Mesquita, G. kauan R. Dantas, E. R. Silva, V. C. Falcone De Oliveira, H. M. Rezende, G. M. Frota, M. Cavalcante, J. R. C. Garcês, M. Souza de Andrade and M. do S. Cartagenes, *Food Sci. Nutr.*, 2025, **13**, e70938, DOI: 10.1002/fsn3.70938.
29 L. R. Ellis, S. Zulfiqar, M. Holmes, L. Marshall, L. Dye and C. Boesch, *Nutr. Rev.*, 2022, **80**, 1723–1737, DOI: 10.1093/nutrit/nuab104.
30 C. M. Mandaji, R. da Silva Pena and R. C. Chisté, *Food Res. Int.*, 2022, **151**, 110820, DOI: 10.1016/j.foodres.2021.110820.
31 I. Da-Costa-Rocha, B. Bonnlaender, H. Sievers, I. Pischel and M. Heinrich, *Food Chem.*, 2014, **165**, 424–443, DOI: 10.1016/j.foodchem.2014.05.002.
32 M. I. Gamal El-Din, E. M. Mantawy, R. S. Said, N. M. Fahmy, S. Fayez, M. I. Shahin, M. Nasr, A. M. Elissawy and A. N. B. Singab, *Arch. Pharm.*, 2024, **357**, e2400392, DOI: 10.1002/ardp.202400392.
33 T. Sholika Sari, T. E. Munandar, H.-I. Chang, I. Sholikhah and R. Widyowati, *Trends Sci.*, 2025, **22**, 10166, DOI: 10.48048/tis.2025.10166.
34 A. M. Eid, H. Al-Hawari, S. Nazzal and S. Khudarieh, *BMC Complement. Med. Ther.*, 2025, **25**, 47, DOI: 10.1186/s12906-025-04804-2.
35 International Conference On Harmonisation (Ich), *Stability Testing Of New Drug Substances And Products Q1A(R2)*, 2003.
36 International Conference On Harmonisation (Ich), *Evaluation For Stability Data Q1E*, 2003.
37 B. S. Mammadov, *International Biotechnology Congress*, Istanbul, Türkiye, 2020: p. PS-001.
38 B. S. Mammadov, *Mod. Achiev. Azerb. Med.*, 2020, **2**, 77–83.
39 B. S. Mammadov and S. D. Mehralieva, *Azerbaijan Pharm. Pharmacother. J.*, 2021, **202100042/25**, 25.
40 A. A. Öztürk and A. Aygül, *J. Res. Pharm.*, 2020, **24**, 110–111, DOI: 10.35333/jrp.2020.115.
41 A. A. Öztürk, İ. Namlı and A. Aygül, *Assay Drug Dev. Technol.*, 2021, **19**, 156–175, DOI: 10.1089/adt.2020.1014.
42 G.-W. Oh, S. Y. Nam, S.-J. Heo, D.-H. Kang and W.-K. Jung, *Int. J. Biol. Macromol.*, 2020, **156**, 1565–1573, DOI: 10.1016/j.ijbiomac.2019.11.206.
43 S. Mehraliyeva, B. Mammadov, M. Valiyeva, *Scientific Collection "InterConf"/11th International Scientific and Practical Conference Scientific Horizon in the Context of Social Crises*, InterConf Scientific Publishing Center, Tokyo, Japan, 2022, 103.
44 S. S. Vaghani, M. M. Patel, C. S. Satish, K. M. Patel and N. P. Jivani, *Curr. Drug Deliv.*, 2012, **9**, 628–636, DOI: 10.2174/156720112803529837.
45 A. A. Öztürk, U. M. Güven and E. Yenilmez, *Acta Pharm. Sci.*, 2018, **56**, 81–105, DOI: 10.23893/1307-2080.aps.05627.
46 A. A. Öztürk and U. M. Güven, *J. Res. Pharm*, 2019, **23**, 426–440, DOI: 10.12991/jrp.2019.150.
47 A. A. Öztürk, E. Yenilmez, R. Arslan, B. Şenel and Y. Yazan, *J. Res. Pharm.*, 2020, **24**, 82–99, DOI: 10.35333/jrp.2020.114.
48 J. F. S. Fernando, C. Zhang, K. L. Firestein and D. Golberg, *Small*, 2017, **13**, 1701564, DOI: 10.1002/smll.201701564.
49 Z. Jafarifar, M. Rezaie, P. Sharifan, V. Jahani, S. Daneshmand, H. Ghazizadeh, G. A. Ferns, S. Golmohammadzadeh and M. Ghayour-Mobarhan, *Appl. Biochem. Biotechnol.*, 2022, **194**, 914–929, DOI: 10.1007/s12010-021-03656-z.

© 2026 The Author(s). Published by the Royal Society of Chemistry

50 J. Song, H. Wang, Y. Yang, Z. Xiao, H. Lin, L. Jin, Y. Xue, M. Lin, F. Chen, M. Zhu, Y. Zhao, Z. Qiu, Y. Li and X. Zhang, *J. Mater. Sci. Mater. Med.*, 2018, **29**, 84, DOI: 10.1007/s10856-018-6094-9.

51 A. A. Öztürk and C. Arpagaus, *Assay Drug Dev. Technol.*, 2021, **19**, 412–441, DOI: 10.1089/adt.2021.053.

52 H. M. Bayomy, D. P. T. Blackmore, E. S. Alamri, N. A. Ozaybi, S. E. Almasoudi, S. Pearson, L. Eyouni, N. A. AlFaris, G. M. Alshammari, M. Muhammed and M. A. Mohamady Hussein, *Int. J. Biol. Macromol.*, 2025, **305**, 141241, DOI: 10.1016/j.ijbiomac.2025.141241.

53 S. Mehraliyeva and E. Babayev, *InterConf*, 2022, **20**, 267–275, DOI: 10.51582/interconf.19-20.04.2022.027.

54 A. Imbriano, M. Mendico, S. Primavilla, M. Carafa, L. Perioli, M. Ricci, A. Di Michele, C. Viseras, C. Pagano, F. G. Villén and R. de Melo Barbosa, *J. Drug Deliv. Sci. Technol.*, 2025, **111**, 107151, DOI: 10.1016/j.jddst.2025.107151.

55 S. Alshehri and S. S. Imam, *Drug Deliv*, 2021, **28**, 2348–2360, DOI: 10.1080/10717544.2021.1995078.

56 W. A. Mahdi, S. I. Bukhari, S. S. Imam, S. Alshehri, A. Zafar and M. Yasir, *Pharmaceutics*, 2021, **13**, 1087, DOI: 10.3390/pharmaceutics13071087.

57 A. K. Philip, N. Singh and K. Pathak, *Pharm. Dev. Technol.*, 2009, **14**, 540–547, DOI: 10.1080/10837450902832893.

58 R. Malviya, Green approach for fabrication of chitosan-neem gum polyelectrolyte stabilized penta and hexagonal nanoparticles and in-vitro cytotoxic potential toward breast cancer (MCF -7) cells, *Precis. med. sci.*, 2020, **9**, 68–82, DOI: 10.1002/prm2.12025.

59 Z. Zhang, B. Zhang, R. Chen, Q. Zhang and K. Wang, *Pharmaceutics*, 2025, **17**, 513, DOI: 10.3390/pharmaceutics17040513.

60 N. Ahmadi, P. J. Ahranjani and L. Rashidi, *Food Sci. Nutr.*, 2025, **13**, e70781, DOI: 10.1002/fsn3.70781.

61 P. Gasner, D. Babusca, A. Vleoanga and D. O. Dorohoi, *Symmetry*, 2025, **17**, 1739, DOI: 10.3390/sym17101739.

62 M. Ekinci, A. A. Öztürk and D. İlem Özdemir, *J. Res. Pharm.*, 2022, **26**, 1636–1645.

63 R. H. Müller, K. Mäder and S. Gohla, Solid lipid nanoparticles (SLN) for controlled drug delivery–a review of the state of the art, *Eur. J. Pharm. Biopharm.*, 2000, **50**, 161–177, DOI: 10.1016/s0939-6411(00)00087-4.

64 S. Kongtaveesombat, S. Torgbo, N. Kamonsutthipaijit, B. Wanikorn and P. Sukyai, *Sci. Rep.*, 2026, **50**, 5530, DOI: 10.1038/s41598-026-35333-8.

65 A. Espona-Noguera, J. Ciriza, A. Cañibano-Hernández, L. Fernandez, I. Ochoa, L. Saenz del Burgo and J. L. Pedraz, *Int. J. Biol. Macromol.*, 2018, **107**, 1261–1269, DOI: 10.1016/j.ijbiomac.2017.09.103.

66 J. Zhang, J. Han, A. Zhu, X. Zhu, Y. Zeng, M. Yin, Y. Xiao, C. Wang, C. Yin, X. Wang, G. Zhang and C. Hao, *J. Biomed. Mater. Res. A.*, 2025, **113**, e37936, DOI: 10.1002/jbm.a.37936.

67 A. Pachauri, H. Chitme, S. Visht, V. Chidrawar, N. Mohammed, B. A. Abdel-Wahab, M. M. Khateeb, M. S. Habeeb, M. A. A. Orabi and M. B. Bakir, *Gels*, 2023, **9**, 209, DOI: 10.3390/gels9030209.

68 M. Hoque, R. P. Babu, C. McDonagh, S. Jaiswal, B. K. Tiwari, J. P. Kerry and S. Pathania, *Int. J. Biol. Macromol.*, 2024, **271**, 132414, DOI: 10.1016/j.ijbiomac.2024.132414.

69 N. T. Muliawati, D. Siswanta and N. H. Aprilita, *Indones. J. Chem.*, 2020, **21**, 411, DOI: 10.22146/ijc.56759.

70 A. A. Öztürk, E. Başaran, B. Şenel, M. Demirel and Ş. Sarıca, *J. Mol. Struct.*, 2023, **1282**, 135169, DOI: 10.1016/j.molstruc.2023.135169.

71 D. Suvakanta, N. M. Padala, N. Lilakanta and C. Prasanta, *Acta Pol. Pharm.*, 2010, **67**, 217–223.

72 J. Zuo, Y. Gao, N. Bou-Chacra and R. Löbenberg, *Biomed. Res. Int.*, 2014, **2014**, 204925, DOI: 10.1155/2014/204925.

73 Y. Zhang, M. Huo, J. Zhou, A. Zou, W. Li, C. Yao and S. Xie, *AAPS J.*, 2010, **12**, 263–271, DOI: 10.1208/s12248-010-9185-1.

© 2026 The Author(s). Published by the Royal Society of Chemistry